Rutaecarpine ameliorates osteoarthritis by inhibiting PI3K/AKT/NF-κB and MAPK signalling transduction through integrin αVβ3

JUNLAI WAN[1,2*], MENGWEI LI[1*], XI YUAN[1], XIAOJUN YU[1], ANMIN CHEN[1], MING SHAO[3], HAO KANG[1] and PENG CHENG[1]

[1]Department of Orthopaedics, Tongji Hospital, Tongji Medical College, Huazhong University of Science and Technology, Wuhan, Hubei 430030; [2]Division of Spine Surgery, Department of Orthopedic Surgery, Nanjing Drum Tower Hospital, Affiliated Hospital of Medical School, Nanjing University, Nanjing, Jiangsu 210008; [3]Department of Orthopaedics, The Third Affiliated Hospital of Guangzhou Medical University, Guangzhou, Guangdong 510530, P.R. China

Received November 6, 2022; Accepted August 3, 2023

DOI: 10.3892/ijmm.2023.5300

Abstract. Osteoarthritis (OA) is a chronic progressive articular illness which commonly affects older-aged adults, presenting with cartilage inflammation and degradation. Rutaecarpine (RUT) has been shown to exert promising anti-inflammatory effects; however, the efficacy of RUT in the treatment of OA is debatable. The present study investigated the potential of RUT in alleviating OA in a mouse model. Treatment with RUT inhibited the inflammatory response and extracellular matrix degradation by suppressing process regulators in interleukin (IL)-1β-stimulated chondrocytes. Moreover, treatment with RUT *in vitro* upregulated the gene expression of anabolic agents, such as collagen type II, aggrecan and SRY-box transcription factor 9, indicating that RUT contributed to cartilage repair. Additionally, flow cytometric assays, and the measurement of β-galactosidase levels, autophagic flux and related protein expression revealed that RUT effectively attenuated IL-1β-induced chondrocyte apoptosis, senescence and autophagy impairment. In addition, bioinformatics analysis and *in vitro* experiments demonstrated that RUT protected cartilage by mediating the phosphoinositide-3-kinase (PI3K)/Akt/nuclear factor-κB (NF-κB) and mitogen-activated protein kinase (MAPK) pathways. The ameliorative effects of RUT on IL-1β-stimulated chondrocytes were abrogated when siRNA was used to knock down integrin αVβ3. Furthermore, the results of immunohistochemical analysis and microcomputed tomography confirmed the *in vivo* therapeutic effects of RUT in mice with OA. On the whole, the present study demonstrates that RUT attenuates the inflammatory response and cartilage degradation in mice with OA by suppressing the activation of the PI3K/AKT/NF-κB and MAPK pathways. Integrin αVβ3 may play a pivotal role in these effects.

Correspondence to: Professor Peng Cheng or Dr Hao Kang, Department of Orthopaedics, Tongji Hospital, Tongji Medical College, Huazhong University of Science and Technology, 1095 Jiefang Avenue, Wuhan, Hubei 430030, P.R. China
E-mail: peng_cheng987@163.com
E-mail: 2010tj0625@hust.edu.cn

*Contributed equally

Abbreviations: RUT, rutaecarpine; OA, osteoarthritis; COX2, cyclooxygenase-2; IL-1β, interleukin-1β; MMP3, matrix metalloproteinases; SOX9, SRY-box transcription factor 9; CCK-8, Cell Counting Kit-8; KEGG, Kyoto Encyclopedia of Genes and Genomes; MAPK, mitogen-activated protein kinase; PI3K/AKT/NF-κB,phosphoinositide-3-kinase/Akt/nuclearfactor-κB; RT-qPCR, reverse transcription-quantitative polymerase chain reaction; H&E, haematoxylin and eosin; OARSI, Osteoarthritis Research Society International

Key words: rutaecarpine, osteoarthritis, integrin αVβ3, PI3K/AKT/NF-κB, MAPK

Introduction

Osteoarthritis (OA) is a chronic degenerative arthropathy hallmarked by cartilage degeneration, inflammatory response, space narrowing and osteophyte formation (1). OA progression can lead to articular synovitis, meniscus rupture, varus deformity and even disability (2). The increased incidence of OA poses an enormous burden on global health and economic development. An imbalance between articular cartilage metabolic effects is the main cause of progressive OA. Moreover, inflammation is a key risk regulator of OA development. Artificial joint replacement is almost the sole intervention therapy for advanced-stage OA (3). Although non-steroidal anti-inflammatory drugs are clinically prescribed to relieve OA, they have limited efficacy and cause an increased clinical risk of gastrointestinal peptic ulcers and cardiovascular diseases (4-8). Therefore, the development of safe and effective clinical drugs to ameliorate osteoarthritis is urgently required.

Studies have demonstrated the presence of metabolic disorders in patients with osteoarthritis, such as the low expression of collagen type II (COL II) and aggrecan, and the

high expression of matrix metalloproteinases (MMPs) (9,10). In addition, previous studies have indicated that the progression of OA is accompanied by hollow cartilage lacunae and hypocellularity, indicating the occurrence of chondrocyte senescence and death, demonstrating their roles in the development of OA (11,12). As OA progresses, cell death is complex as it involves apoptosis, senescence, oxidative stress, chondroptosis, necrosis and autophagy (11,12). Accordingly, autophagy activation, antioxidation, antisenescence and decreased apoptosis serve as therapeutic strategies against the progression of OA.

Previous studies have confirmed the crucial role of the activation of the nuclear factor-κB (NF-κB) pathway in the interleukin (IL)-1β-induced inflammatory response and OA progression (4,13,14). An IL-1β stimulus induces the phosphorylation of Akt, which further phosphorylates IκBα, displaying the nuclear localization signal on the NF-κB complex. Consequently, the stimulation and translocation of the NF-κB p65 subunit (p65) into the nucleus triggers downstream gene transcription. Therefore, Akt phosphorylation triggers the downstream phosphorylation of p65 and IκBα. NF-κB is a vital signalling substance for the phosphoinositide-3-kinase (PI3K)/Akt pathway (4,15,16), which comprises several serine/threonine protein kinases. Thus, the classic PI3K/Akt/NF-κB pathway contributes to the progression of OA and is considered a primary target for the treatment of OA.

Mitogen-activated protein kinases (MAPKs) are serine/threonine kinases, such as p38, extracellular signal-regulated kinase (ERK)1/2 and c-Jun N-terminal kinase (JNK). It has been demonstrated that the MAPK signalling pathway, which transmits inflammatory cellular signals to facilitate inflammation, markedly contributes to articular cartilage degradation (17). Moreover, MAPK phosphorylation is linked to the expression level of MMPs, which cause the deterioration of aggrecan and COL II. Furthermore, the inhibition of MAPKs downregulates the IL-1β-induced activity of cyclooxygenase (COX)2 and prostaglandin E2 in chondrocytes (17).

Rutaecarpine (RUT), a novel drug of the class 'COX2 inhibitors' and an indolopyridoquinazoline alkaloid isolated from *Evodia rutaecarpa* (18), has been shown to exert inhibitory effects against inflammation. RUT has been shown to inhibit Kelch-like ECH-associated protein 1-nuclear factor erythroid 2-related factor 2 (Nrf2) binding to trigger Nrf2 and attenuate dextran sulfate sodium-induced colitis (19). Furthermore, RUT has been found to inhibit prostaglandin synthesis in macrophages (20) and mitigate inflammation in RAW 264.7 macrophages by reducing PI3K/Akt/NF-κB and MAPK signal transduction (21). The potential value of RUT in the synovitis of rheumatoid arthritis has also been reported (22). Moreover, it has been shown to effectively inhibit the apoptosis and production of inflammatory cytokines in neuronal injury by regulating the signal transduction of the Nrf2/heme oxygenase-1 and ERK1/2 pathways (23). In addition, a previous study demonstrated that RUT effectively inhibited osteoclastogenesis by impairing macrophage colony stimulating factor and receptor activator of nuclear factor κ-B ligand-stimulated signalling pathways (24). Thus, RUT has exhibited various pharmacological effects, such as anti-inflammatory, anti-apoptotic and antioxidant effects. However, whether RUT can alleviate murine osteoarthritis remains unexplored. Hence, the present study aimed to examine the curative effects of RUT on IL-1β-activated murine chondrocytes.

Materials and methods

Chemicals, reagents and antibodies. RUT (CAS 84-26-4) was purchased from Shandong Topscience Biotech Co., Ltd. and its molecular structure is illustrated in Fig. 1A. Recombinant mouse IL-1β cytokine was obtained from R&D Systems, Inc. (401-ML-010) and Safranin O solution was obtained from Beijing Solarbio Science & Technology Co., Ltd. (cat. no. G1067). Corresponding primary antibodies against COL II (cat. no. 28459-1-AP), SOX9 (cat. no. 67439-1-Ig), aggrecan (cat. no. 13880-1-AP) and MMP13 (cat. no. 18165-1-AP) were acquired from Proteintech Group, Inc. and used at a 1:1,000 dilution. GAPDH monoclonal antibody (cat. no. 60004-1-Ig, Proteintech Group, Inc.) was used at a 1:50,000 dilution. Wuhan Boster Biological Technology, Ltd. provided the primary antibodies against MMP3 (cat. no. BM4074, 1:1,000), trypsin, as well as the reagents, collagenase type II and phosphate-buffered saline (PBS), HRP-AffiniPure goat anti-rabbit IgG (1:10,000; cat. no. BM3894), HRP-AffiniPure goat anti-mouse IgG (1:10,000; cat. no. BM3895) and CY3-conjugated AffiniPure goat anti-rabbit IgG (1:200; cat. no. BA1032) for western blot analysis and immunofluorescence analyses. Cell Signalling Technology, Inc. provided the corresponding primary antibodies against COX2 (cat. no. 12282), BAX (cat. no. 14796), BCL2 (cat. no. 3498), autophagy-related 5 (ATG5, cat. no. 12994) and microtubule-associated protein light chain 3 (LC3I/II, cat. no. 12741), and constituents of the MAPK and PI3K/Akt/NF-κB pathways: p38 (cat. no. 8690), phosphorylated (p-)p38 (cat. no. 4511), ERK1/2 (cat. no. 4695), p-ERK (#4370), JNK (cat. no. 9258), p-JNK (cat. no. 9255), PI3K (cat. no. 4257), p-PI3K (cat. no. 4228), AKT (cat. no. 4691), p-AKT (cat. no. 4060), p65 (cat. no. 8242) and p-p65 (cat. no. 3033); all these antibodies were used at a 1:1,000 dilution. A primary antibody against p21 (cat. no. ab188224, 1:1,000) was acquired from Abcam. p16 (INK4A) antibody (cat. no. A0262, 1:750) was purchased from ABclonal Biotech Co., Ltd. Rabbit antibodies against TNF-α (cat. no. 48136) and IL-6 (cat. no. 32064) were acquired from Signalway Antibody and used at a 1:1,000 dilution. The Annexin V-FITC/PI Apoptosis Detection kit was acquired from Vazyme Biotech Co., Ltd. The senescence β-galactosidase staining kit was purchased from the Beyotime Institute of Biotechnology. LC3 autophagy double-labelled adenovirus (cat. no. HBAD-1007) was purchased from HanBio Inc. In addition, Gibco; Thermo Fisher Scientific, Inc. provided foetal bovine serum (FBS) and Dulbecco's modified Eagle's medium F12 (DMEM/F12).

Chondrocyte extraction and culture. As previously described, chondrocytes were obtained from the knee joints of sacrificed C57BL/6J mice (5 days old) by sequential enzymatic digestion (25). The total knee cartilage was extracted and placed in PBS. The synovium and other attachments were stripped thoroughly from the cartilage surface. Subsequently, the separated cartilage was crumbled into miniature patches and immersed in 0.25% trypsin for digestion in a cell incubator for 30 min 37˚C. The sediment was transferred and regurgitated

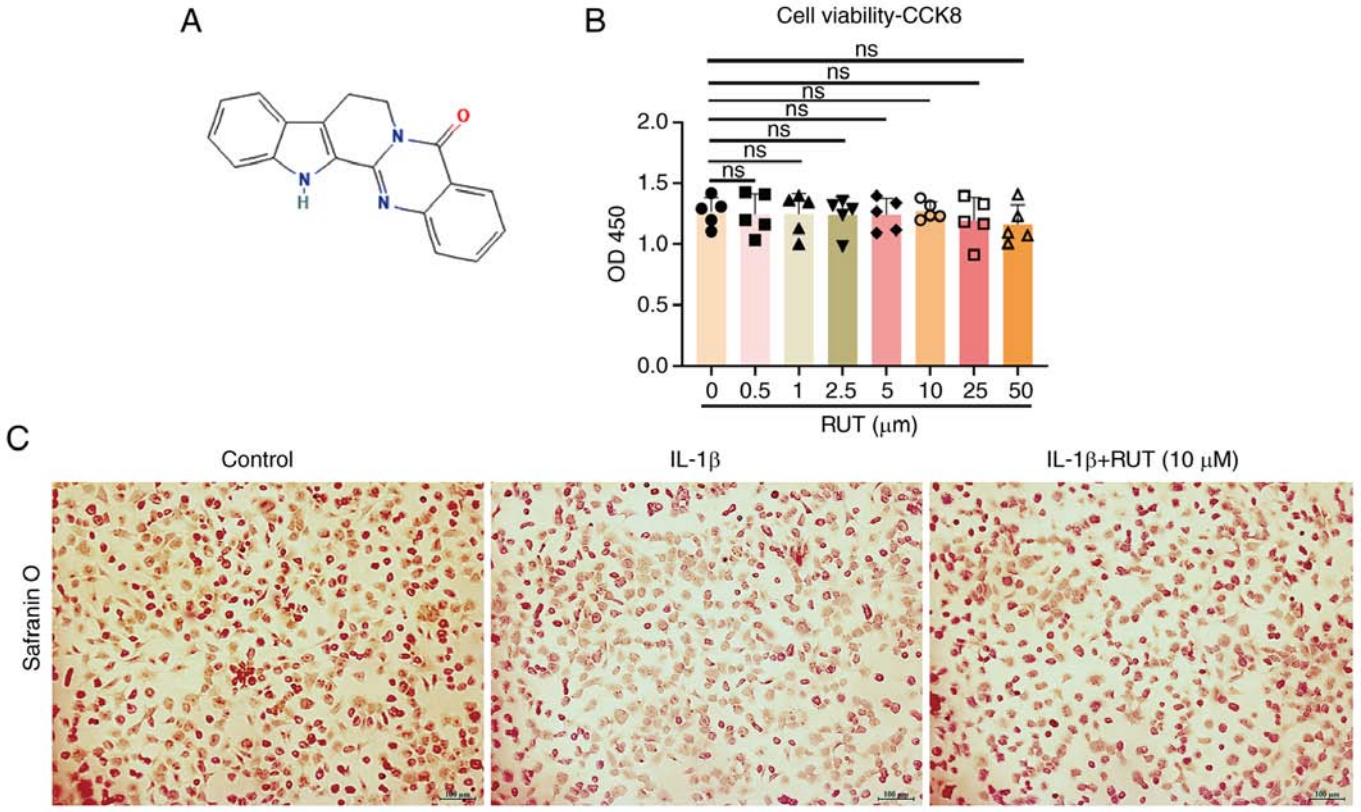

Figure 1. Identification of mouse chondrocytes and the effects of RUT on mouse chondrocyte viability. (A) Molecular structure of RUT. (B) Mouse chondrocytes were treated with RUT (0, 1, 2.5, 5 and 10 μM) for 24 h, and examined using the Cell Counting Kit-8 assay. The values are presented as the mean ± SD of three independent experiments. (C) Safranin O staining of primary mouse chondrocytes stimulated with IL-1β (5 ng/ml) and RUT (5 or 10 μM) for 24 h (scale bar, 100 μm). ns, no significant difference (P>0.05). IL-1β, interleukin 1 β; RUT, rutaecarpine.

with 0.2% collagenase II for 6 h in a hybridization oven at 37˚C after being centrifuged at 362 x g for 5 min 37˚C. The chondrocyte sediment was then isolated from suspension by centrifugation at 362 x g for 5 min 37˚C and cultured in a medium including 10% FBS, 1% penicillin/streptomycin and DMEM/F12 culture medium in a cell incubator. Matured chondrocytes were collected for subsequent *in vitro* evaluation.

Cell viability assay. The Cell Counting Kit-8 (CCK-8) (cat. no. AR1199, Wuhan Boster Biological Technology, Ltd.) was employed to detect the cytotoxic action of a graded concentration of RUT on mouse chondrocytes that were seeded and cultured for a day using a 96-well plate at a density of 5,000 to 10,000 cells per well. Following cell treatment using a concentration gradient of RUT (0, 1, 2.5, 5 and 10 μM) for 1 day, 100 μl of the mixture (containing 10 μl CCK-8 reagent) were added and the chondrocytes were incubated for 1 h at 37˚C in the dark. Subsequently, a microplate reader (Bio-Rad Laboratories, Inc.) was used to detect the cell absorbance at 450 nm wavelength.

Safranin O staining of cells. Safranin O staining was used to relatively quantify the proteoglycan content. The chondrocytes seeded into six-well plates were treated with IL-1β (5 ng/ml) (9,25) for 1 day with/without RUT (5 or 10 μM) when the cells reached 80% confluency. PBS was used to wash the cells three times, and the cells were then stabilized using 4% paraformaldehyde (PFA) at room temperature for 30 min prior to incubation with Safranin O reagent for 2 h at 37˚C, followed by dye removal and washing with PBS. A light microscope was used to capture the brightness of Safranin O/fast green staining (EVOS FL auto, Life Technologies; Thermo Fisher Scientifc, Inc.).

Western blot analysis. The chondrocytes seeded in six-well plates were placed on ice, and the culture medium was discarded, followed by washing with PBS three times. The cell lysate was prepared following the thorough drying of the plates using filter paper. The cells were lysed with lysis buffer comprised radioimmunoprecipitation assay (RIPA) lysis buffer, phosphatase and protease inhibitors at a ratio of 100:1:1 (Wuhan Boster Biological Technology, Ltd.). Following cell lysis on ice for 20 min, the cells mixed with lysate were scraped off using cell wipers and collected. The mixture was fully crushed using an ultrasonic crusher (Sonicator Q125, Qsonica, LLC.) and centrifuged at 16,099 x g for 30 min at 4˚C. Following centrifugation, the protein concentration in the supernatant was measured using BCA assay (Wuhan Boster Biological Technology, Ltd.). The supernatants were mixed with loading buffer (4:1), refrigerated for 5 min and denatured at 95˚C for 10 min, leading to the final protein samples. These were then subjected to sodium dodecyl sulphate-polyacrylamide gel electrophoresis (8.0-12.5%) and transferred onto a polyvinylidene difluoride membrane. Subsequently, 5% bovine serum albumin (Wuhan Boster Biological Technology, Ltd.) was then employed to denature the membrane sites for 1 h at 25˚C. The membranes

were then incubated with specific primary antibodies at 4˚C overnight, rinsed three times using Tris-buffered saline with 0.1% Tween®-20 for 15 min, incubated at room temperature with specific secondary antibodies for 1 h, and then washed three times for 15 min each time with the same saline and buffer mixture. Finally, the target protein bands were exposed using enhanced chemiluminescence (Abbkine), saved using Image Lab™ Software v.4.0 (Bio-Rad Laboratories, Inc.) and quantified using ImageJ software v.1.8.0 (National Institutes of Health).

Reverse transcription-quantitative polymerase chain reaction (RT-qPCR). RT-qPCR was performed to evaluate the expression levels of inflammatory cytokines in the RUT-treated chondrocytes. The chondrocytes were plated into a six-well plate and cultured with medium containing IL-1β (5 ng/ml) for 1 day with/without RUT (5 or 10 μM). The extraction of total RNA was performed using the Total RNA kit I (Omega Bio-tek) according to the manufacturer's instructions. Complementary DNA (cDNA) synthesis was executed using a Rever Tra Ace qPCR RT kit (cat. no. FSQ-101, Toyobo Life Science), and subsequently amplified using a RT-qPCR kit [cat. no. 13117ES, Yeasen Biotechnology (Shanghai) Co., Ltd.] on a Bio Rad Q5 instrument (Bio-Rad Laboratories, Inc.) under the following conditions: 5 min at 95˚C, and thereafter 40 cycles of 10 sec at 95˚C and 30 sec at 60˚C. The relative levels of target gene expression were normalized to the internal reference gene, GAPDH. The results were quantified using the relative $2^{-\Delta\Delta Cq}$ method (26). The sequences of the primers used for RT-qPCR are presented in Table I.

Table I. Primer sequences used in RT-qPCR.

Gene	Sequence
GAPDH	F: 5'-CCCAGCTTAGGTTCATCAGG-3'
	R: 5'-ATCTCCACTTTGCCACTGC-3'
IL-6	F: 5'-CCTTCCTACCCCAAT TTCCAAT-3'
	R: 5'-GCCACTCCTTCTGTGACTCCAG-3'
TNF-α	F: 5'-ATGTCTCAGCCTCTTCTC-3'
	R: 5'-GCCATTTGGGAACTTCTC-3'
Integrin αV	F: 5'-AATAAGATCTGCCCGTTGCC-3'
	R: 5'-GTAGAAGCTCCACCTGGAAG-3'
Integrin β3	F: 5'-TGATG GGCACTGTCACATTG-3'
	R: 5'-TTCTGGTAAAGGCTGACGAC-3'

F, forward; R, reverse; IL-6, interleukin 6.

Immunofluorescence staining. Confocal dishes were prepared for COL II and p65 staining, and the chondrocytes were evenly seeded at $2x10^4$ per dish and cultured for 24 h. These cells were then stimulated with IL-1β (5 ng/ml) for 24 h with/without RUT (10 μM). Subsequently, 4% PFA was used to fix the plates for 30 min at 25˚C, followed by rinsing with 0.2% Triton X-100 for 15 min. The unbound sites on the plates were then blocked using 1% bovine serum albumin for 30 min at normal temperature. Subsequently, primary antibodies against COL II (1:200; cat. no. 28459-1-AP, Proteintech Group, Inc.) and p65 (1:400; cat. no. 8242, Cell Signaling Technology, Inc.) were used to incubate the cells at 4˚C overnight. Following a wash with PBS, the chondrocytes were incubated with Cy3-conjugated Affinipure goat anti-rabbit secondary antibody (1:200; cat. no. BA1032, Wuhan Boster Biological Technology, Ltd.) for 1 h at room temperature in the dark. The chondrocyte nuclei were then subjected to staining using 4',6-diamidino-2-phenylindole (cat. no. AR1176, Wuhan Boster Biological Technology, Ltd.) for 10 min at room temperature in the dark. A confocal microscope (Nikon Corporation) was used for screening and obtaining images.

Senescence β-galactosidase staining. β-galactosidase activity was evaluated using a senescence β-galactosidase staining kit. The chondrocytes seeded into six-well plates were treated for 1 day with IL-1β (5 ng/ml) with/without RUT (10 μM). The plate was then triple-washed with PBS, stabilized in 4% PFA for 15 min at room temperature, incubated with the mixture staining fluid at 37˚C overnight without CO_2, and finally observed under a light microscope (EVOS FL auto, Life Technologies; Thermo Fisher Scientific, Inc.). The density of the senescent cells was measured using ImageJ software v.1.8.0 (National Institutes of Health) as the cell count (cells with blue spots).

Apoptosis evaluation. Flow cytometric analysis was utilized to calculate the chondrocyte apoptotic rates. The chondrocytes were seeded in six-well plates and cultured in an integrated medium containing 10% FBS, 1% penicillin/streptomycin and DMEM/F12 culture medium (Thermo Fisher Scientific, Inc.). When the cells reached 80% confluency, they were treated with IL-1β (5 ng/ml), and treated with or without RUT (1, 2.5, 5 and 10 μM) for 1 day, digested using trypsin, rinsed using PBS and resuspended in 100 μl binding buffer for 5 min. Subsequently, 5 μl FITC Annexin V and 10 μl propidium iodide from the Annexin V-FITC/PI apoptosis kit were combined with the suspension without light at room temperature for 5-10 min. Subsequently, 400 μl binding buffer were added, and finally, a flow cytometer was used to detect the apoptotic cells (Moflo XDP, Beckman Coulter) and FlowJo v10 software (FlowJo LLC) was used to analyse the apoptotic cells.

mRFP-GFP-LC3 adenovirus infection and confocal microscopy. LC3 protein was overexpressed using mRFP-GFP-LC3 autophagy double-labelled adenovirus (HanBio Inc.) and labelled with red and green fluorescence to observe the autophagic flux. The chondrocytes were seeded in confocal dishes and incubated in complete medium consisting of 10% FBS, 1% penicillin/streptomycin and DMEM/F12 culture medium (Thermo Fisher Scientific, Inc.). When the cells reached approximately 50% confluency, adenoviral vectors (HanBio Inc.) were used to infect them at a formerly defined multiplicity of infection (MOI) of 20 for 1 day (9). IL-1β (5 ng/ml) was then used to treat the cells with/without RUT (10 μM) for 24 h. Subsequently, the autophagic flux was recorded using a confocal microscope (Nikon Corporation). Due to acid sensitivity, the green fluorescence was quenched following autolysosome formation, and only red fluorescence could be detected. The number of green and red nodes was

recorded to evaluate the intensity of autophagy and the number of autophagosomes, respectively.

Bioinformatics analysis of potential mechanisms of RUT intervention in OA. Predicted RUT target genes were acquired from the PharmMapper database and then input into the Database for Annotation, Visualization, and Integrated Discovery (DAVID) to obtain RUT-related Kyoto Encyclopedia of Genes and Genomes (KEGG) pathways. Simultaneously, OA-related pathways were screened from the miRWalk2.0 database (http://mirwalk.umm.uni-heidelberg.de/). The KEGG pathways of RUT-target genes were intersected with the OA-related pathways to obtain common pathways by Venn Diagram (Venny2.1). RNA-seq data were obtained from the Gene Expression Omnibus (GEO) database (accession no. GSE210476) (27), and the R package ggplot2 was used for quantitative analysis of gene-level expression. A molecular docking analysis was performed using Autodock Vina on RUT (C18H13N3O) and integrin αVβ3 (PDB: 6MSL). PyMOL (https://pymol.org/2/) was used to visualize the docking of molecules.

siRNA. Specific integrin αV (ItgαV) and β3 (Itgβ3) siRNAs (Table II) were synthesized by Guangzhou Ribobio Co., Ltd. with two repeats of each siRNA to knock down integrins αV and β3. The chondrocytes seeded in six-well plates were transfected with negative control or siRNA against integrins αV and β3 (50 nM) using Lipofectamine 3000® reagent (Thermo Fisher Scientific, Inc.) and Opti-MEM (Gibco; Thermo Fisher Scientific, Inc.) at 37˚C for 24 h. The knockdown efficiency of each repeat was examined using RT-qPCR as described above. Subsequently, the repeat with the highest effectivity of ItgαV and Itgβ3 siRNA was used to transfect the chondrocytes for 24 h to confirm the amelioration of osteoarthritis by RUT in the presence or absence of integrin αVβ3.

Histological staining and immunohistochemical analysis. RUT was intra-articularly injected at a dose of 25 mg/kg per week following the establishment of a destabilization of the medial meniscus (DMM) model using mice, as described below. After 2 months, all mice were sacrificed to obtain their right knee joints. The soft tissue of the joints was thoroughly removed, and the joints were immersed in 4% PFA (Wuhan Boster Biological Technology, Ltd.) at room temperature for 1 day, decalcified in 10% ethylenediaminetetraacetic acid for 30 days and embedded in paraffin. In addition, 5-μm-thick sections were sliced for tissue staining and immunohistological evaluation. Haematoxylin and eosin (H&E), Safranin O/fast green, and toluidine blue (Beijing Solarbio Science & Technology Co., Ltd.) were used for tissue section staining following the corresponding protocols [staining at room temperature; haematoxylin (5 min) eosin (1 min), Safranin (2 min), fast green (5 min), toluidine blue (30 min)]. Images were obtained using an Olympus BX63 microscope (Olympus Corporation). The degree of mouse cartilage damage was determined according to the Osteoarthritis Research Society International (OARSI) guidelines (28). Following deparaffinization and blocking with 5% bovine serum albumin at 37˚C for 1 h, the sections were incubated overnight at 4˚C using primary antibodies against the anabolic factor, aggrecan (1:200; cat. no. 13880-1-AP), and the catabolic factor, MMP13 (1:100; cat. no. 18165-1-AP) (both from Proteintech Group, Inc.). HRP-AffiniPure goat anti-rabbit IgG (1:500; cat. no. BM3894, Wuhan Boster Biological Technology, Ltd.) was then incubated with the sections at 37˚C for 1 h, followed by development and observation under an Olympus BX63 microscope (Olympus Corporation).

Table II. siRNA sequences used for siRNA assays.

siRNA	Sequence
ItgαV siRNA#1	GAGGATCTCTTCAACTCTA
ItgαV siRNA#1	ACCCGTTGTCACTGTAAAT
ItgαV siRNA#1	GCAAGAAAGAGAACAGCTT
Itgβ3 siRNA#1	CCGTGAATTGTACCTACAA
Itgβ3 siRNA#1	GCTGATGACTGAGAAACTA
Itgβ3 siRNA#1	CCATGACCGGAAGGAATTT
Negative control siRNA	TTCTCCGAACGTGTCACGT

Itg, integrin.

Animal experiments. The present study was conducted as per the approval and regulations of the Ethics and Animal Research Committee of Huazhong University of Science and Technology [(2021) IACUC no. 2908]. A total of 60 C57BL/6J mice (6-8 weeks old, male) were supplied by the Experimental Animal Centre of Tongji Hospital and fed with normal chow and water in an SPF animal laboratory at 25˚C with 12:12 light/dark cycle. The mice were randomly divided into three groups (the control, OA and OA + RUT groups). Following inhalation-induced anaesthesia with 2% isoflurane and maintenance with 1.5% isoflurane, the model of DMM was constructed in the OA and OA + RUT groups by cutting at the joint cavity and transecting the anterior medial meniscus-tibial ligament to immobilize the medial meniscus, as previously described (4,9,10,15). The mice in the control group underwent joint cavity opening and only anterior fat pad excision. A 1 week after the surgery, the articular cavity of the mice in the OA + RUT group was injected with a 10-μl solution of RUT at 25 mg/kg per week for 8 weeks. Simultaneously, the mice in the control and OA group were administered 10 μl saline solution. Following the completion of the intra-articular injection course, the mice were sacrificed by cervical dislocation following deep anaesthesia with 5% isoflurane, and the right knee joints were obtained and subjected to further evaluation. The three-dimensional reconstruction and the evaluation of bone volume fraction (BV/TV), trabecular separation (TB.Sp) and trabecular number (TB.N) were all performed using the micro-computed tomography system (μ-CT50, SCANCO Medical AG).

Statistical analysis. The experimental data analysed using GraphPad Prism v.8.4.0 (Dotmatics). The outcomes are presented as the mean ± SD. The Student's t-test was employed to compare two groups to highlight their variations. One-way analysis of variance (ANOVA) with Tukey's post hoc test were employed to compare two or more groups. A P-value <0.05 was considered to indicate a statistically significant difference. All analyses were repeated independently at least three times.

Results

Cell viability and identification of mouse chondrocytes. The viability of the chondrocytes treated with various concentrations of RUT (0, 1, 2.5, 5 and 10 μM) for 24 h was detected using a CCK-8 kit. As shown in Fig. 1B, RUT did not exert any significant cytotoxic effects on the chondrocytes; therefore, the 1, 2.5, 5 and 10 μM concentrations of RUT were chosen for use in further experimentations. Furthermore, Safranin O staining was conducted to observe chondrocyte morphology. A mild loss of staining was observed in the IL-1β-stimulated chondrocytes that was reversed by RUT treatment in a concentration-dependent manner. The proteoglycan content revealed that RUT administration promoted anabolism in chondrocytes (Fig. 1C).

RUT attenuates the IL-1β-induced expression of inflammatory mediators and catabolic factors and reverses the IL-1β-induced degeneration of anabolic factors in mouse chondrocytes. COX2, IL-6, TNF-α and IL-1β are major inflammatory cytokines and their levels are enhanced in IL-1β-stimulated chondrocytes (4,17). To determine the anti-inflammatory effects of RUT, chondrocytes that reached 80% confluency were treated with various concentrations of RUT with/without IL-1β (5 ng/ml) for 1 day, and the cell lysate was subjected to western blot analysis and RT-qPCR. As shown in Fig. 2A and C-E, a marked elevation in the expression levels of the aforementioned proteins was observed in the chondrocytes stimulated by IL-1β, and the increasing pattern was averted in a concentration-dependent manner by RUT. Additionally, the present study evaluated the mRNA expression levels of inflammatory cytokines in chondrocytes with or without RUT treatment when IL-1β (5 ng/ml) was used for 24 h. As illustrated in Fig. 2D and E, RUT significantly suppressed the mRNA expression of IL-6 and TNF-α induced by IL-1β. Moreover, as COL II, aggrecan and SOX9 are highly significant anabolic enzymes with crucial roles in maintaining extracellular matrix (ECM) cartilage homeostasis, the expression of these proteins was determined to analyse the anabolism level in chondrocytes. The results revealed an attenuation in COL II, aggrecan and SOX9 production by IL-1β, and the suppressive trend was mitigated by RUT in a concentration-dependent manner (Fig. 2B and F). Furthermore, the expression levels of catabolic enzymes were significantly augmented in the IL-1β-stimulated chondrocytes, indicating the disruption of ECM homeostasis. The expression of the key chondrocyte catabolic indicators, MMP3 and MMP13, was examined to verify the beneficial effects of RUT on IL-1β-stimulated chondrocytes from mice with OA. As shown in Fig. 2B and G, IL-1β abnormally upregulated MMP-3 and MMP-13 expression. The IL-1β-stimulated chondrocytes treated with RUT exhibited a concentration-dependent decrease in catabolic enzyme expression. In addition, the immunofluorescence analysis of COL II revealed similar changes following the treatment of IL-1β-stimulated chondrocytes with/without RUT (Fig. 2H).

RUT attenuates IL-1β-induced senescence and apoptosis, and impairs chondrocyte autophagy. Chondrocyte senescence occurs with OA progression, with inflammation as the primary process regulator (11). The activity of β-galactosidase, a critical enzyme, regulates cell senescence (9). Herein, the expression of β-galactosidase markedly increased in the IL-1β-stimulated chondrocytes compared to the normal chondrocytes for 24 h, and treatment with RUT (10 μM) effectively mitigated β-galactosidase activity (Fig. 3A and B). Consistent with this phenomenon of enhanced expression with IL-1β stimuli and its reversal in the presence of RUT, a similar effect was observed in the activity of senescence marker proteins, including p16 (INK4A) and p21 in chondrocytes (Fig. 3C and D). Additionally, the expression of BCL2 (an anti-apoptotic protein) and BAX (a pro-apoptotic protein) was determined using western blot analysis. Consistent with the findings of a previous study (1), stimulation with IL-1β for 24 h significantly augmented BAX activity and reduced BCL2 expression in the chondrocytes (Fig. 3G and H). However, these effects were effectively reversed in a concentration-dependent manner by RUT.

Furthermore, the results of flow cytometric analysis (Fig. 3E and F) demonstrated that the rate of apoptosis increased in chondrocytes stimulated with IL-1β for 1 day and decreased following treatment with RUT in a concentration-dependent manner. These data collectively demonstrated the potential anti-apoptotic effects of RUT on IL-1β-stimulated chondrocytes. Furthermore, the expression of autophagy-related proteins and the autophagic flux were determined to verify whether the ameliorating effects of RUT on mouse OA involved autophagy. The results of western blot analysis revealed that the inhibition of proteins linked to autophagy, including LC3I/II and ATG5, under IL-1β stimulation (Fig. 3K and L) was reversed by RUT in a concentration-dependent manner. Moreover, treatment with RUT (10 μM) enhanced the number of autophagosomes and autolysosomes in contrast to the group stimulated with IL-1β for 24 h (Fig. 3I and G). Thus, RUT may have a potential ameliorating effect on impaired autophagy in chondrocytes.

Bioinformatics analysis of the potential therapeutic mechanisms of RUT. Based on the PharmMapper database, the potential target genes of RUT were identified using bioinformatic methods. KEGG pathway enrichment analysis was used to enrich 151 pathways to analyse RUT target genes. The PI3K/Akt, proteoglycans in cancer, prostate cancer and MAPK signalling pathways constituted the top four pathways with the greatest number of genes (Fig. 4A). Simultaneously, 43 common pathways were obtained via the intersection of OA-related pathways and KEGG pathways of RUT target genes (Fig. 4B), which may potentially underlie the therapeutic mechanisms of RUT. The data obtained from RNA sequencing (GSE210476) were analysed in primary human macrophages treated with or without lipopolysaccharide (LPS; 100 ng/ml) and RUT (10 μM) (27). The gene expression of integrin β3 markedly increased in the RUT-treated macrophages compared to the LPS-stimulated groups for 24 h (Fig. 4C). An intervention with RUT increased the expression of integrin β3. Hence, integrin β3 might be a potential target gene of RUT. With the assistance of AutoDock Vina, a ligand docking analysis was conducted to further investigate the possible interaction modes between RUT and integrin β3. A docking analysis revealed that the RUT protein formed three hydrogen bond interactions with the amino acids in the integrin β3 protein, which had a strong association (Fig. 4D).

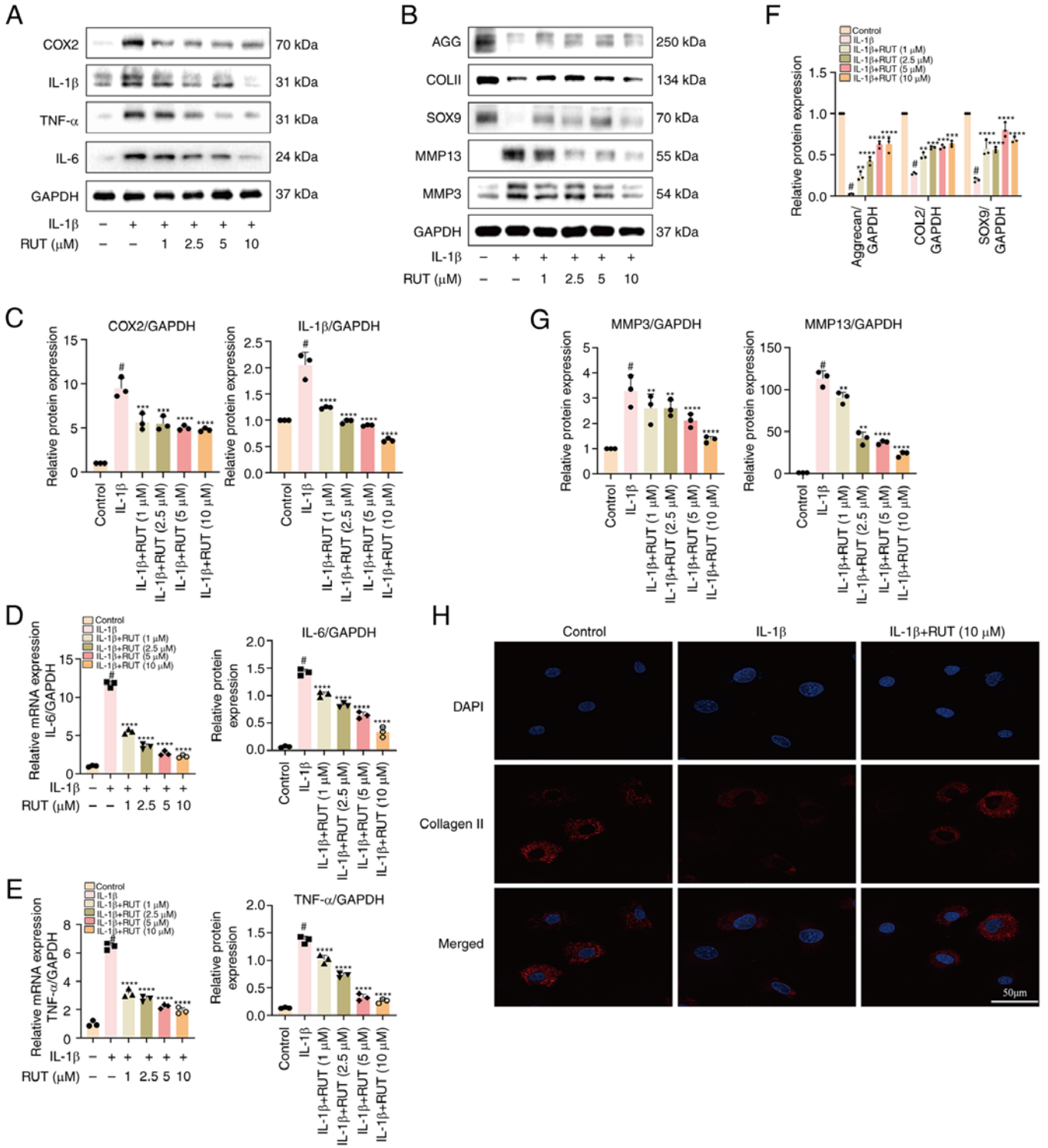

Figure 2. Protective effects of RUT against IL-1β-induced inflammation and extracellular matrix degradation in mouse chondrocytes. The cells were exposed to IL-1β (5 ng/ml) with/without RUT (1, 2.5, 5 and 10 μM) for 24 h. (A and B) The protein expression levels of MMP3, MMP13, IL-1β, COX2, IL-6, TNF-α, SOX9, COL II and aggrecan were determined using western blot analysis. (C-G) Quantification analysis of the results of western blotting. (D and E) Relative mRNA expression levels of IL-6 and TNF-α in chondrocytes stimulated with IL-1β (5 ng/ml) and treated with or without RUT (1, 2.5, 5 and 10 μM) for 24 h. The values are presented as the mean ± SD of three independent experiments. $^{\#}$P<0.05 vs. control group; **P<0.01, ***P<0.001 and ****P<0.0001 vs. IL-1β group. (H) The protein expression of COL II was detected using immunofluorescence following treatment of the cells with IL-1β (5 ng/ml) with/without RUT (10 μM) for 24 h. IL-1β, interleukin 1 β; RUT, rutaecarpine; MMP, matrix metalloproteinase; COX2, cyclooxygenase 2; SOX9, SRY-box transcription factor 9; COL II, collagen type II.

RUT mitigates the activation of the PI3K/Akt/NF-κB and MAPK pathways in mouse chondrocytes stimulated with IL-1β. According to the prediction results of bioinformatics analysis, the PI3K/AKT and MAPK pathways were regarded as two potential mechanisms of the effects of RUT on OA occurrence and progression, as they are closely associated with inflammation, metabolism and autophagy (18). The chondrocytes were treated with RUT in a concentration gradient for 1 day and then

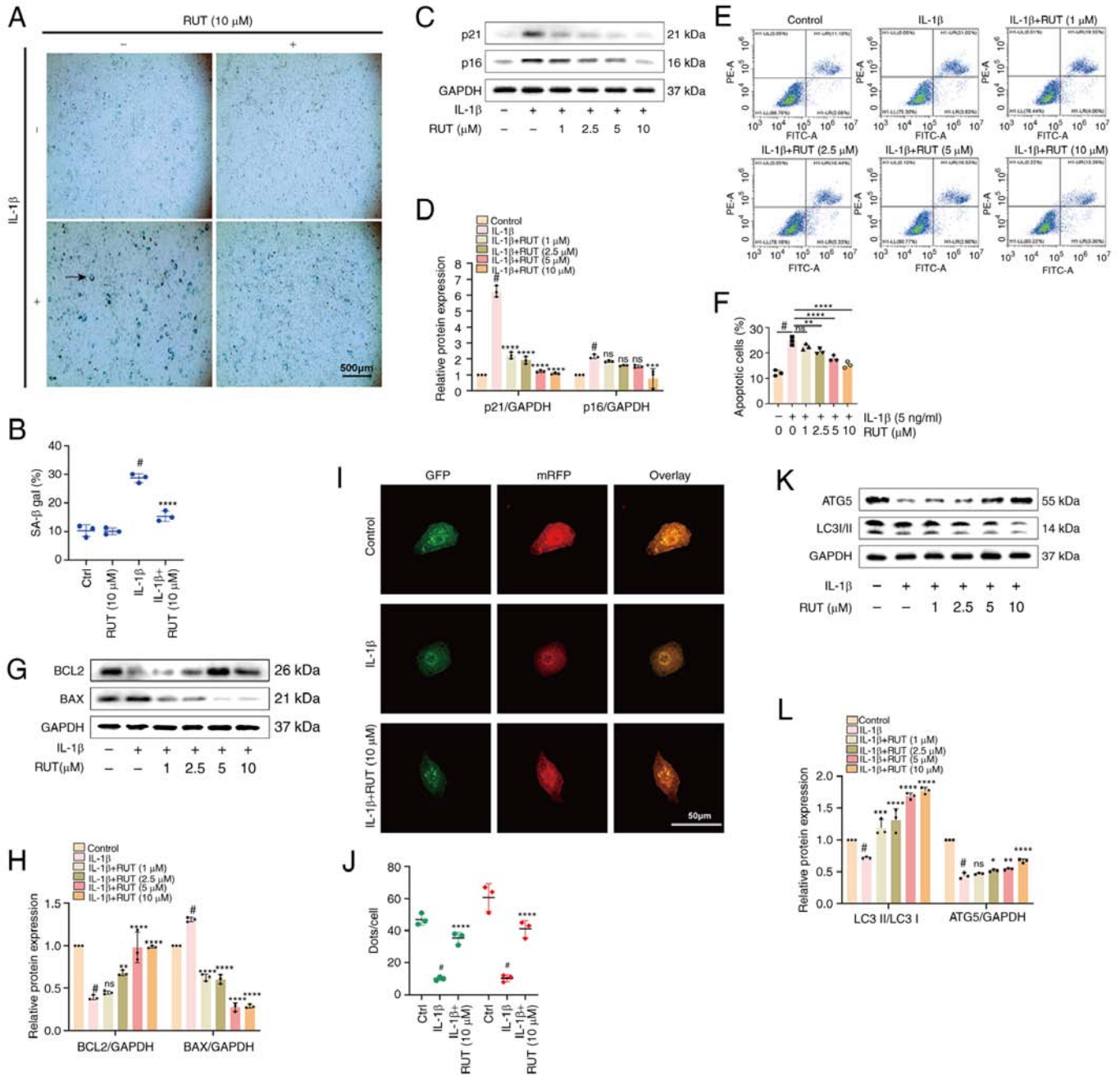

Figure 3. Effects of RUT on IL-1β-induced chondrocyte senescence, apoptosis and autophagy. The cells were stimulated with 5 ng/ml IL-1β in the presence or absence of RUT (10 μM) for 24 h. (A) β-galactosidase staining of chondrocytes. Scale bar, 500 μm. (B) Quantification analysis of β-galactosidase activity. (C and D) Results of western blot analysis of the senescence marker proteins, p21 and p16 (INK4A), and corresponding quantification analysis. (E and F) Apoptotic chondrocytes and corresponding apoptosis rates. (G and H) Levels of the apoptosis-related proteins, BAX and BCL2. (I) Yellow puncta represent autophagosomes, and red puncta represent autolysosomes in the merged images. (J) Quantification analysis of dots/cells. (K and L) The outcomes of western blot analysis and quantification analysis of proteins linked to autophagy (ATG5 and LC3I/II). The values are presentd as the mean ± SD of three independent experiments. $^{\#}$P<0.05 vs. control group; *P<0.05, **P<0.01, ***P<0.001 and ****P<0.0001 vs. IL-1β group; ns, no significant difference (P>0.05). IL-1β, interleukin 1 β; RUT, rutaecarpine; ATG5, autophagy-related 5; LC3, microtubule-associated protein light chain 3.

cultured with/without IL-1β (5 ng/ml) for 30 min. The expression levels of the related proteins in the two aforementioned pathways were determined using western blot analysis. RUT significantly blocked the phosphorylation levels of the related proteins, which indicated that RUT suppressed the activation of the two pathways in a concentration-dependent manner (Fig. 5A-D). Consistent with the results of western blot analysis, immunofluorescence assay demonstrated that RUT interrupted the nuclear translocation of p65 in IL-1β-stimulated chondrocytes (Fig. 5E). These data suggested that RUT alleviated mouse OA by suppressing the stimulation of two signalling pathways.

Alleviating effects of RUT on IL-1β-stimulated chondrocytes are attenuated following the knockdown of integrin αVβ3. The decreasing trend in integrin αV/β3 (ItgαV/β3) levels induced by IL-1β was reversed following treatment of the chondrocyte with RUT, and the knockdown efficiency of the three repeats of siRNA was validated using RT-qPCR (Fig. 6A and B). The

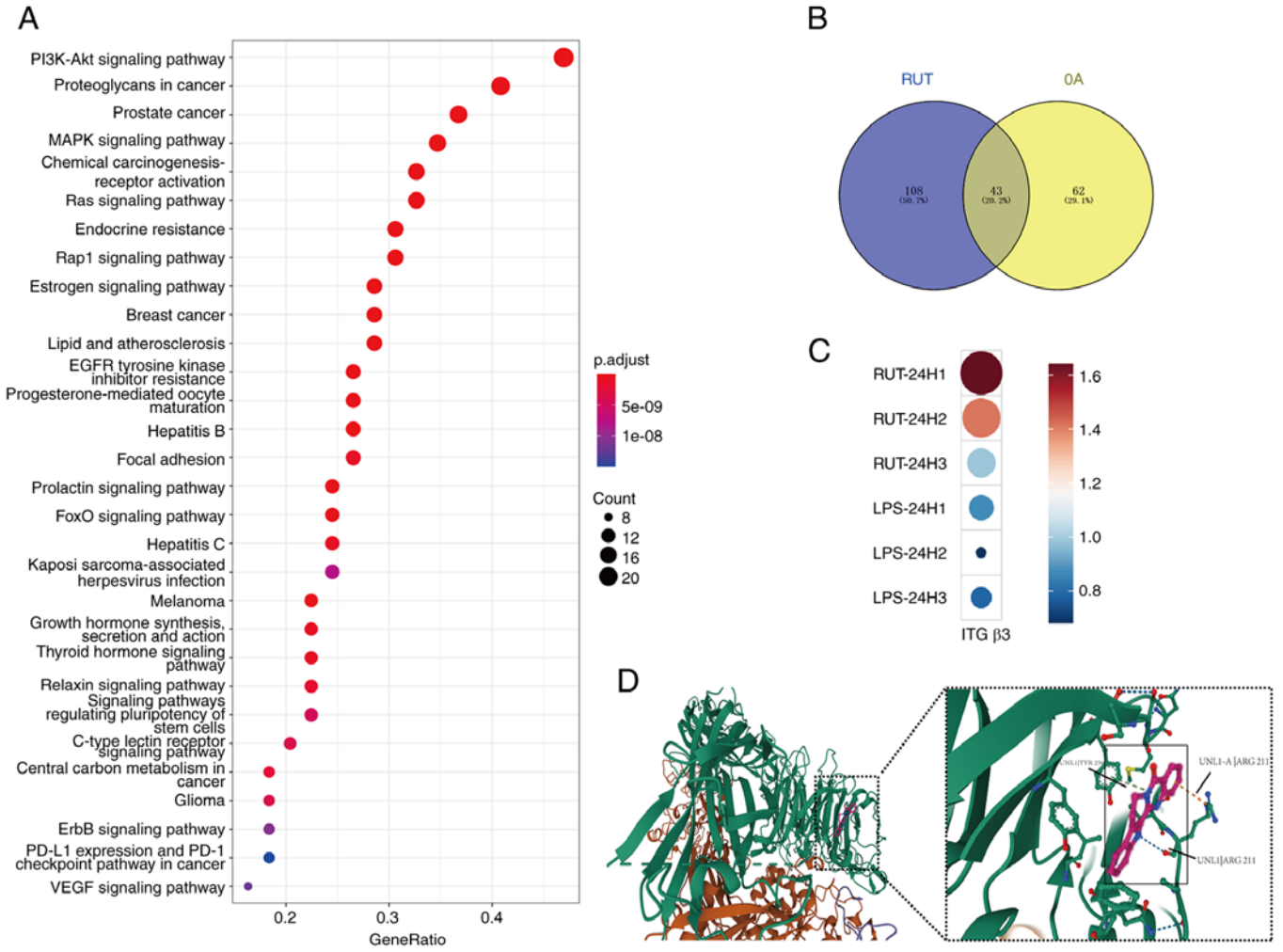

Figure 4. Bioinformatics analysis of the RUT potential target pathways. (A) KEGG pathway enrichment analysis of the RUT target genes. (B) The intersection of RUT KEGG enrichment and osteoarthritis-related pathways (Venn diagram). (C) Heatmap of the gene expression levels of integrin β3 in primary human macrophages stimulated with/without LPS (100 ng/ml) and RUT (10 μM). P<0.05. Raw RNA-seq data were obtained from GSE210476. (D) Docking of RUT with the integrin β3 protein mode. RUT, rutaecarpine; KEGG, Kyoto Encyclopedia of Genes and Genomes; LPS, lipopolysaccharide.

most effective combination was selected: ItgαV siRNA#1 and Itgβ3 siRNA#1 to knock down ItgαV/β3. The chondrocytes were treated only using 5 ng/ml IL-1β; IL-1β with 10 μM RUT; or IL-1β, 10 μM RUT and ItgαV/β3 siRNA. The activity levels of inflammatory, anabolic and catabolic markers were detected using western blot analysis. The results revealed that RUT alleviated OA by enhancing cartilage anabolism, and inhibiting cartilage catabolism and inflammatory markers. This effect was reversed by the knockdown of ItgαV/β3 (Fig. 6C-E and H-M).

3RUT attenuates the destruction of cartilage in vivo in a mouse model of OA. As shown in Fig. 7A, the superficial articular cartilage exhibited more notable abrasion and proteoglycan depletion in the DMM group than in the control group, and the worsening situation was reversed by RUT. A relatively smoother cartilaginous surface and richer proteoglycan were observed in the RUT-treated group than in the untreated DMM group. Furthermore, the calculated OARSI score revealed that RUT administration attenuated the severity of OA (Fig. 7B). Based on the findings of the *in vitro* analysis, the activity of aggrecan and MMP13 exhibited a similar change in the DMM + RUT group. RUT intervention reduced MMP13 synthesis and facilitated aggrecan production (Fig. 7C and D).

RUT attenuates subchondral bone remodelling in vivo in the mouse model of OA. Furthermore, microcomputed tomography was used to examine the effects of RUT on subchondral bone remodelling in a mouse model of OA. The 3D CT images of the right knee from the mice in the control, OA, and OA + RUT groups are presented in Fig. 8A and B. The mice in the OA group exhibited a more significant BV/TV than the control group mice, while a noticeable decrease in TB.Sp was observed and was reversed following treatment with RUT. No statistically significant difference was observed in TB.N between the OA and control groups (Fig. 8C). These findings suggest that RUT had a promising ameliorating effect on subchondral bone remodelling in mice with OA.

Discussion

Previous research has identified the medicinal significance of RUT (19,21,22); however, its role in chondrocytes remains

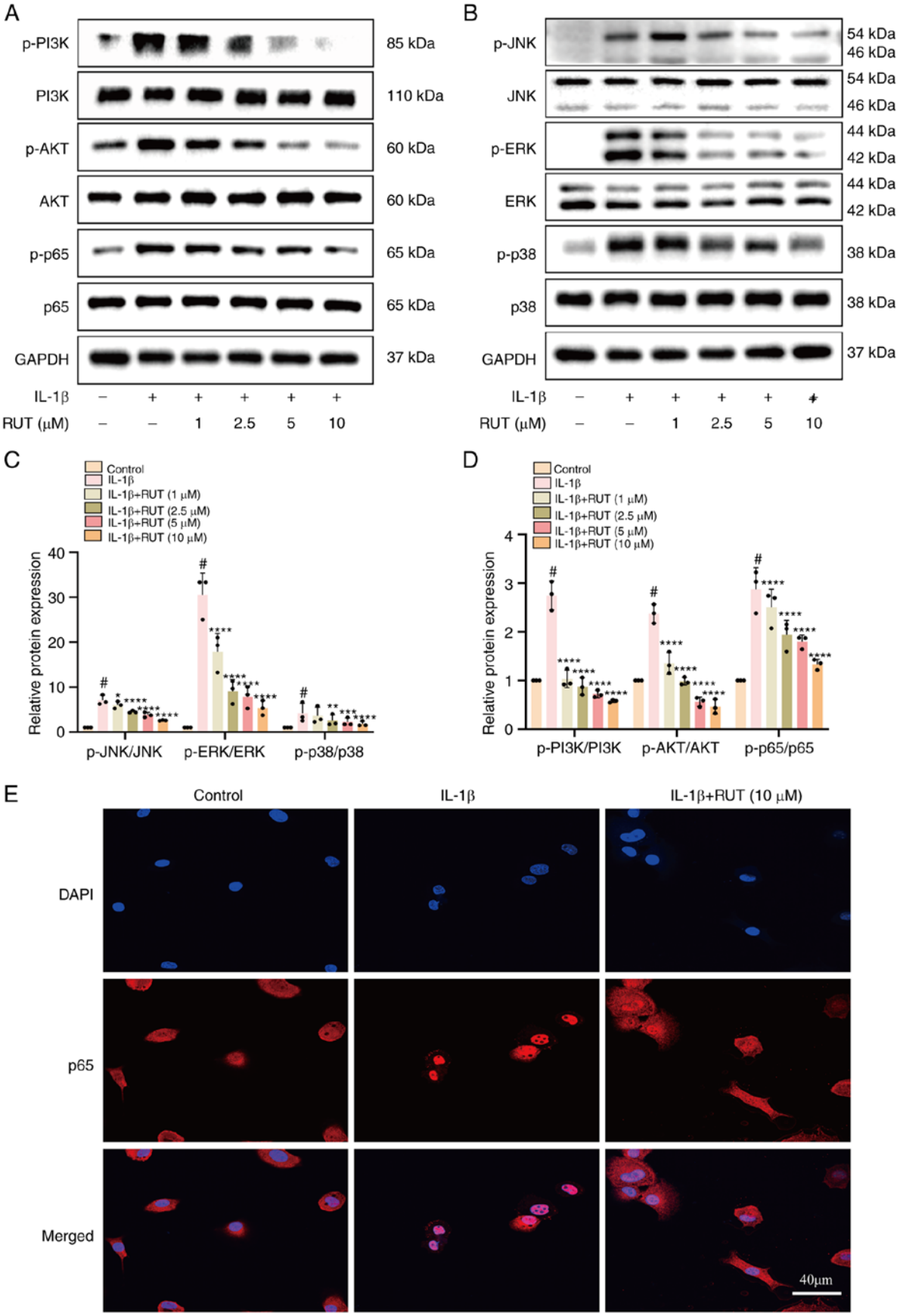

Figure 5. RUT inhibits the activation of PI3K/Akt/NF-κB and MAPK pathways in IL-1β-stimulated chondrocytes. (A and C) Western blot analysis and quantification analysis of PI3K/AKT/NF-κB-related signalling proteins. (B and D) Western blot analysis and quantification analysis of MAPK-related signalling proteins. (E) The protein expression of p65 was detected using immunofluorescence after the chondrocytes were pre-treated with RUT (10 μM) for 24 h and then stimulated with IL-1β (5 ng/ml) for 30 min. The values are presented as the mean ± SD of three independent experiments. $^{\#}$P<0.05 vs. control group; *P<0.05, **P<0.01, ***P<0.001 and ****P<0.0001 vs. IL-1β group. IL-1β, interleukin 1 β; RUT, rutaecarpine; PI3K, phosphoinositide-3-kinase; MAPK, mitogen-activated protein kinase.

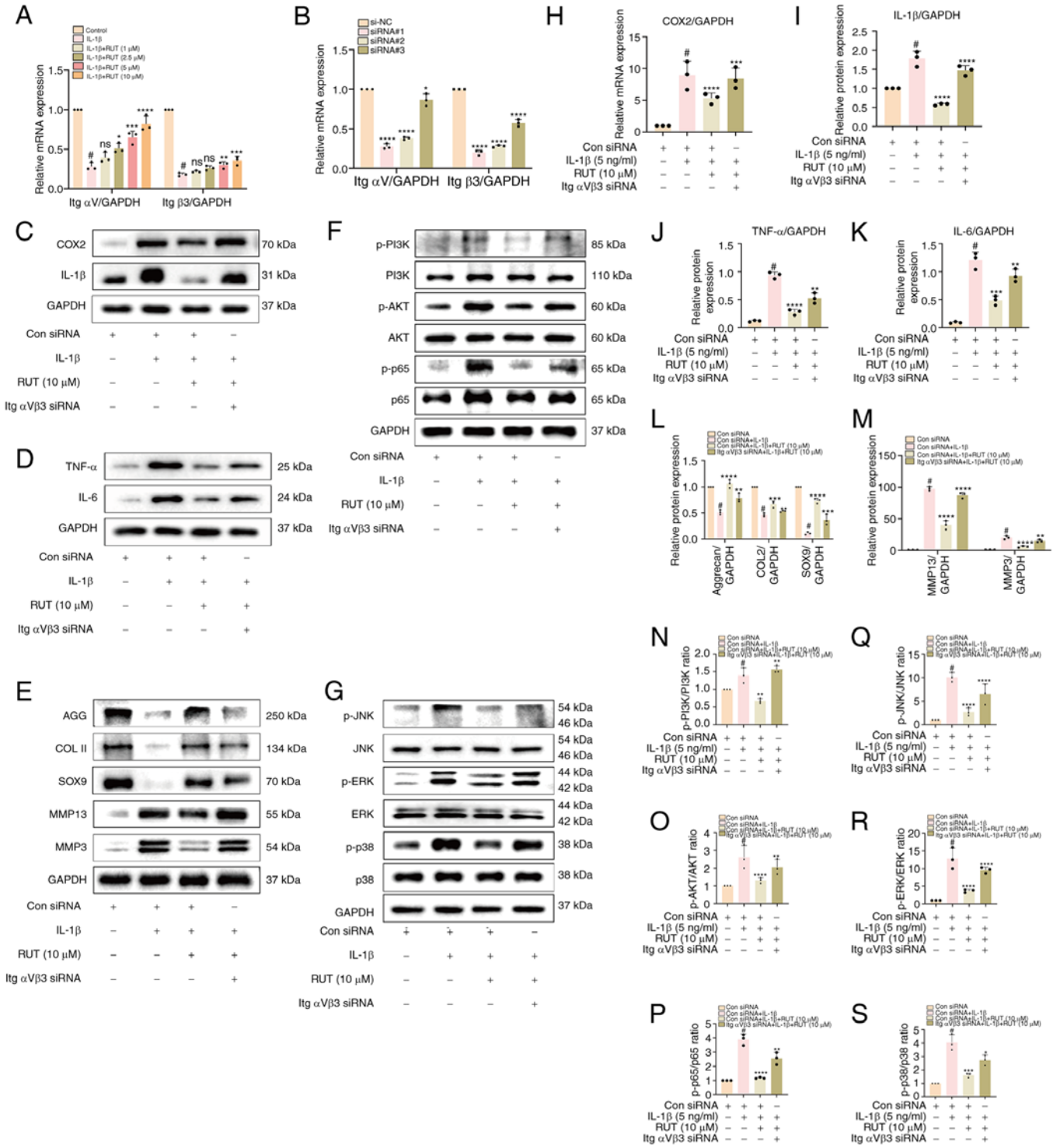

Figure 6. The beneficial effects of RUT on IL-1β-stimulated chondrocytes were attenuated following integrin αVβ3 knockdown. (A and B) Relative mRNA levels of ItgαV and Itgβ3 in chondrocytes exposed to 5 ng/ml IL-1β with/without RUT (1, 2.5, 5 and 10 μM) for 24 h. The knockdown efficiency of ItgαV and Itgβ3 siRNA transfection was verified using RT-qPCR. (C-E and H-M) The expression levels of inflammation and extracellular matrix degradation-related proteins were determined using western blot analysis; the outcomes of the chondrocytes were quantified in the presence/absence of 5 ng/ml IL-1β, RUT (10 μM) and ItgαVβ3 for 24 h. (F and G, and N-S) Western blot analysis and quantification analysis were used to measure the levels of PI3K/Akt/NF-κB and MAPK-related signalling proteins in IL-1β (5 ng/ml)-stimulated chondrocytes for 30 min following transfection with/without ItgαVβ3 siRNA and RUT (10 μM) for 24 h. Data are presented as the mean ± SD of three independent experiments. $^{\#}$P<0.05 vs. control group; *P<0.05, **P<0.01, ***P<0.001 and ****P<0.0001 vs. IL-1β group; ns, no significant difference (P>0.05). IL-1β, interleukin 1 β; RUT, rutaecarpine; MMP, matrix metalloproteinase; COX2, cyclooxygenase 2; SOX9, SRY-box transcription factor 9; PI3K, phosphoinositide-3-kinase; COL II, collagen type II; AGG, aggrecan.

undetermined. In the present study, inflammatory responses were indeed observed in IL-1β-stimulated chondrocytes. However, treatment of the chondrocytes with RUT led to the downregulation of COX2, IL-1β, IL-6 and TNF-α. Additionally, RUT markedly decreased the generation of catabolic enzymes (MMP3 and MMP13) and upregulated

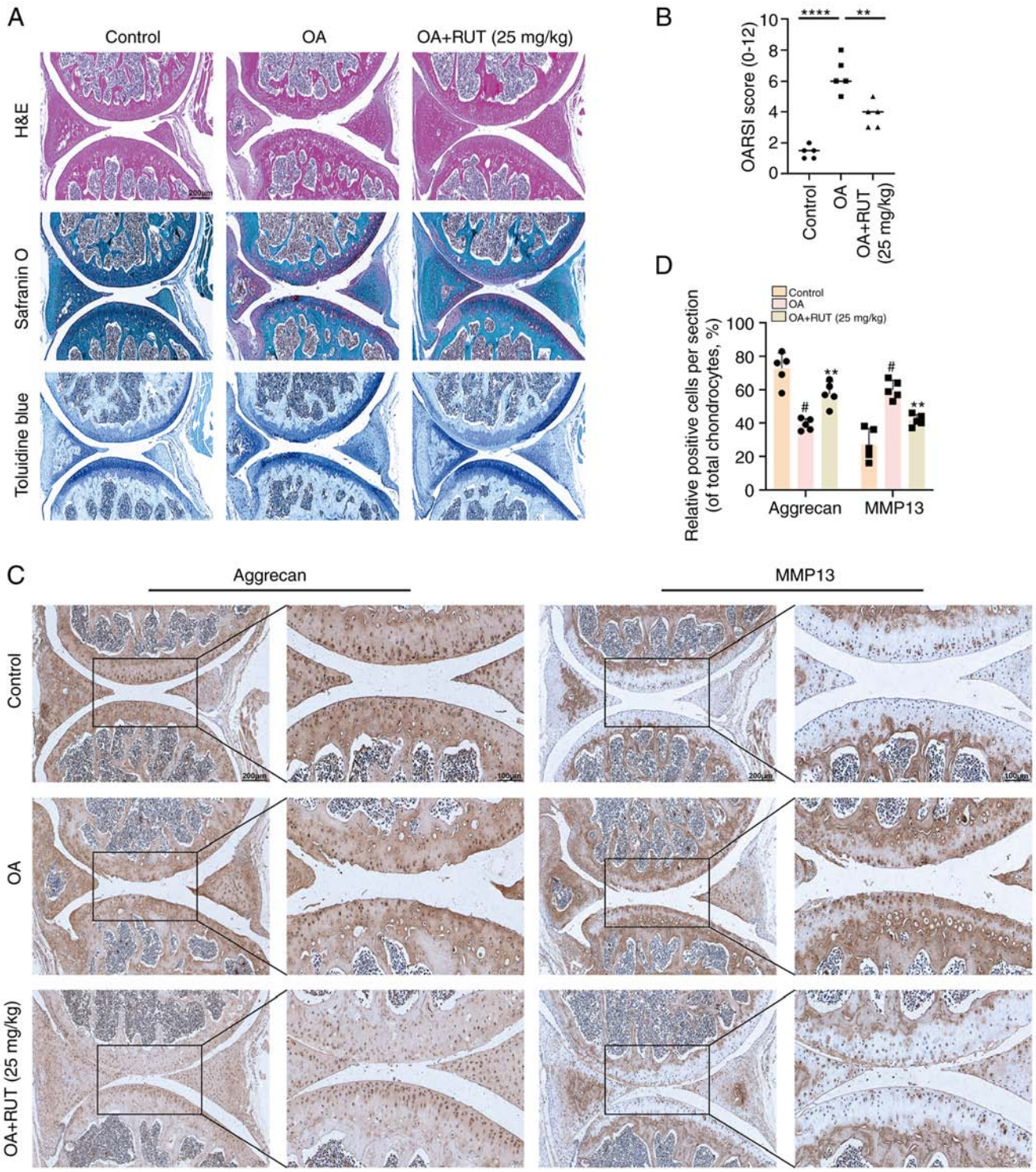

Figure 7. RUT attenuates cartilage destruction *in vivo* in the mouse model of OA. (A) H&E, Safranin O/fast green, toluidine blue staining, and (B) OARSI scores of the mouse knee joints from the control, OA and OA + RUT groups at 8 weeks following the corresponding treatment (scale bars, 100 μm). (C) Immunohistochemical staining and (D) quantification analysis of the expression of aggrecan and MMP13 were conducted among the three groups (scale bars, 50 and 100 μm). Data are presented as the mean ± SD (n=5). $^{\#}$P<0.05 vs. control group; **P<0.01 and ****P<0.0001 vs. OA group. RUT, rutaecarpine; OA, osteoarthritis; OARSI, Osteoarthritis Research Society International; H&E, haematoxylin and eosin; MMP, matrix metalloproteinase.

the expression of anabolic enzymes (COL II, aggrecan and SOX9). The results of immunofluorescence staining confirmed the ameliorating effect, similar to the findings of western blot analysis. These results indicated that RUT promoted anti-inflammation, anti-catabolism and pro-anabolism in chondrocytes. Furthermore, cartilage preservation effects, such as anti-apoptosis, anti-senescence and autophagy repair were also verified in the chondrocytes treated with RUT.

Furthermore, the mutual suppression of the activation of the PI3K/AKT/NF-κB and MAPK signalling pathways by RUT was also observed. Previous research has confirmed that the

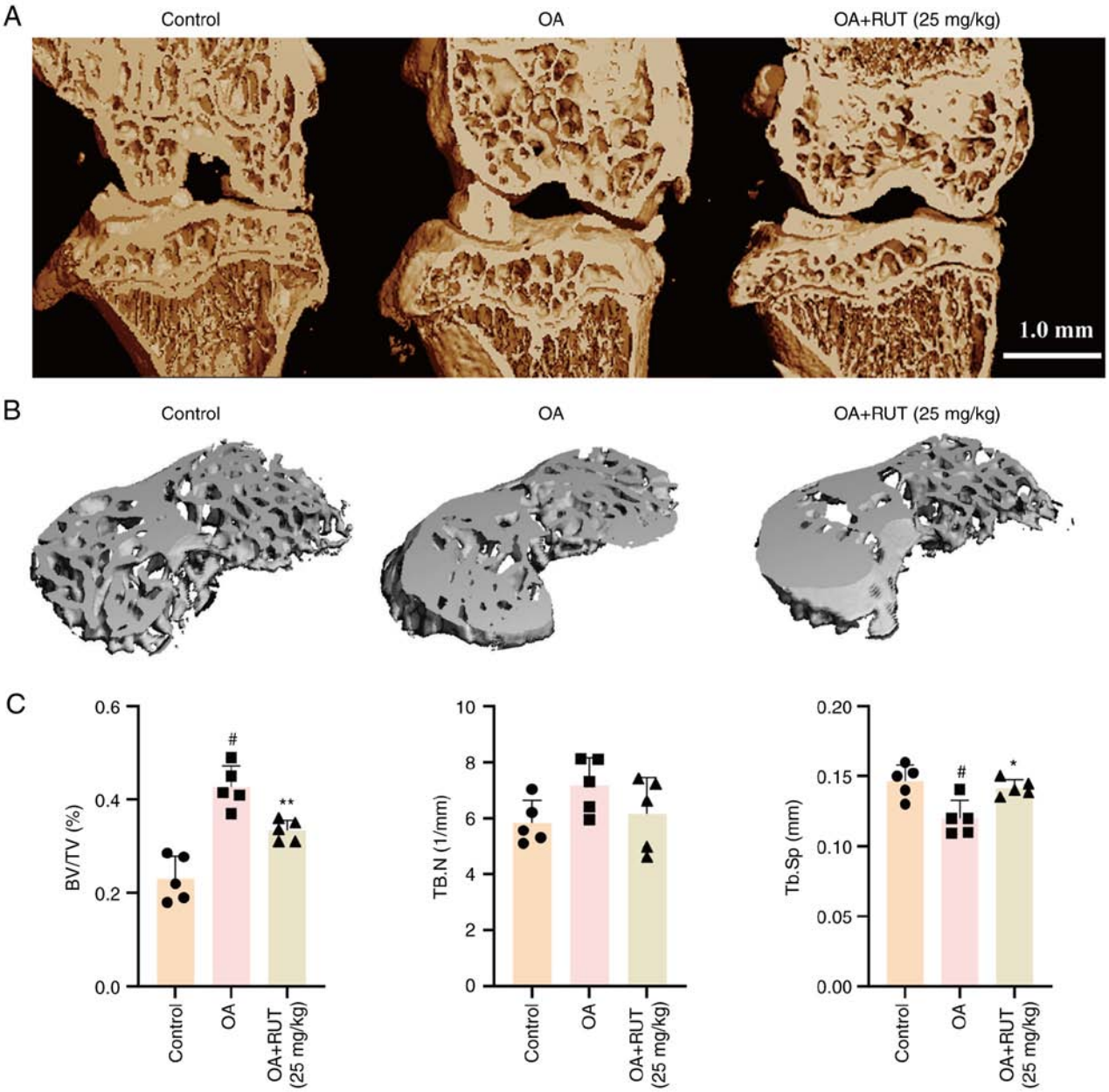

Figure 8. Microcomputed tomography evaluation of the subchondral bone at the tibial plateau *in vivo* in the mouse model of OA. (A and B) Representative images of the 3D microcomputed tomography coronal and cross-sectional views of the right knee from the control, OA and OA + RUT group mice. (C) Histogram plots of the quantification analysis of trabecular structure, including BV/TV, Tb.N and Tb.Sp in the control, OA and OA + RUT group mice. Data are presented as the mean ± SD (n=5). $^{\#}$P<0.05 vs. control group; *P<0.05 and **P<0.01 vs. the OA group. OA, osteoarthritis; RUT, rutaecarpine; BV/TV, bone volume/tissue volume; Tb.N, trabecular number; Tb.Sp, trabecular separation.

rapid activation of PI3K/AKT contributes to the activation of NF-κB (29) and subsequently enhances the expression of COX2. Furthermore, the production of catabolic factors is significantly augmented in OA (30). In the present study, the phosphorylation level of PI3K/Akt/NF-κB in mouse chondrocytes induced by IL-1β was reversed in a concentration-dependent manner by RUT. Moreover, the results of the immunofluorescence staining of p65 confirmed that pre-treatment with RUT impeded the nuclear translocation of NF-κB heterodimers. The aforementioned results strongly indicate that the anti-inflammatory effects of RUT on chondrocytes may be executed by suppressing the activation of the PI3K/Akt/NF-κB signalling pathway. Moreover, the present study revealed that RUT pre-treatment inhibited the IL-1β-mediated phosphorylation of p38, ERK1/2 and JNK in chondrocytes, which suggested that the MAPK signalling pathway may be targeted by RUT for its anti-inflammatory effects.

Integrin αVβ3 is a cell adhesion receptor vital to mediating cellular interaction with the ECM. Previous studies have demonstrated that integrin αVβ3 is expressed in normal adult articular chondrocytes and exerts chondroprotective effects by mitigating the levels of inflammatory factors in IL-1β-stimulated chondrocytes (31,32). Another study suggested that blocking integrin αVβ3 destroyed osteocyte morphology, contributing to inhibition in spread area and process retraction (33). However, a previous study reported the opposite result and stated that integrin αVβ3 was highly active in OA-affected chondrocytes, and its stimulation contributed

to OA progression (34). By contrast, a previous study further revealed that the activation of integrin αVβ3 decreased chondrocyte apoptosis (35). Recently, it was shown that integrin αVβ3 expression was decreased in IL-1β-stimulated chondrocytes, and knocking it down aggravated mouse OA through the stimulation of the two pathways (36). This supported the role of integrin αVβ3 as an upstream target of the aforementioned pathways in OA treatment (36). Another study suggested that integrin αVβ3 has a positive influence on WNT1-inducible-signaling pathway protein 1, protecting rat chondrocytes from senescence and apoptosis (37). In the present study, it was found that there was a positive association between integrin β3 and RUT via RNA-seq data analysis of primary human macrophages treated with or without LPS (100 ng/ml) and RUT (10 μM) from a previous study (27). However, one of the limitations of the present study is that RNA-seq analysis was not performed on chondrocytes treated with IL-1β (5 ng/ml) with/without RUT (10 μM). Therefore, it can only be hypothesized that there may be an association between integrin β3 and RUT in chondrocytes stimulated with IL-1β, and that integrin αVβ3 may be a potential target of RUT in the treatment of OA. Consequently, chondrocytes were transfected with ItgαV and Itgβ3 siRNA to determine the ameliorating effect of RUT on OA in the presence or absence of integrin αVβ3. The findings demonstrated that the knockdown of integrin αVβ3 significantly inhibited the anti-inflammatory, anticatabolic and pro-anabolic effects of RUT on IL-1β-stimulated chondrocytes. Additionally, the inhibition of the PI3K/Akt/NF-κB and MAPK pathways was mitigated following the knockdown of integrin αVβ3. All these outcomes indicated that integrin αVβ3 may be a pivotal factor in the inhibition of OA by RUT.

In the present study, the mouse model of OA exhibited signs of osteophyte hyperplasia, knee joint cartilage abrasion, joint space narrowing and other pathological changes. The histological examination of the mouse knees revealed that RUT treatment decreased articular cartilage impairment in the mouse with OA. Moreover, the results of microcomputed tomography demonstrated that RUT contributed to the remodelling of subchondral bone. Since the protective effects of RUT on OA remained, the present study provides exclusive data confirming the effect of RUT on reducing articular cartilage deterioration in mouse models of OA.

In summary, RUT was found to exert anti-inflammatory and anticatabolic functions in IL-1β-stimulated chondrocytes by suppressing the activation of the PI3K/Akt/NF-κB and MAPK signalling pathways through integrin αVβ3. Collectively, these results emphasize the potential of RUT as a reliable drug for the treatment of OA. However, the findings of the present study need to be expanded upon in the future. The present study was limited to investigating the effects of RUT on OA and did not examine the systemic effects on the body. Intra-articular administration has a number of advantages, including increased local bioavailability, reduced adverse events and reduced costs (38). However, the present study did not investigate the drug retention time and drug metabolism pattern of RUT in the joint cavity. Additionally, due to its potential as an anti-inflammatory agent, it is crucial to understand how RUT promotes cartilage regeneration by mediating OA-related signalling pathways and potential targets of action. Additionally, further research is required to determine whether RUT can improve the progression of OA by acting on other OA-related cells, such as immune cells, following injection into the joint cavity. Studies such as transcriptome sequencing and metabolome sequencing may enable the further understanding of the mechanisms involved in the effects of RUT on OA in the future.

In conclusion, to the best of our knowledge, the present study is the first to reveal the *in vivo* and *in vitro* ameliorating effects of RUT on OA-affected cartilage. These beneficial effects are mediated through anti-inflammatory effects, the suppression of cartilage degradation and the suppression of the PI3K/AKT/NF-κB and MAPK signalling pathways in mice. The cartilage protective effects of RUT on OA may be regulated by integrin αVβ3. RUT or integrin αVβ3 may thus great potential to serve as a drug or molecular targets in the treatment of OA.

Acknowledgements

Not applicable.

Funding

The present study was supported by grants from the National Natural Science Foundation of China (no. 81672168) and the Natural Science Foundation of Hubei Province of China (no. 2020CFB216).

Availability of data and materials

The datasets used and/or analysed during the current study are available from the corresponding author on reasonable request.

Authors' contributions

All authors (JW, ML, XYuan, XYu, AC, MS, HK and PC) were responsible for the reliability of the data sources and the data collation process and analysis operations. The present study was conceptualized and designed by AC, MS, HK and PC. JW, ML, XYuan and XYu performed the experiments. All authors (JW, ML, XYuan, XYu, AC, MS, HK and PC) were involved in data analysis and interpretation. JW and ML participated in the drafting and in the critical revision of the important intellectual content of the article and made significant contributions to the completion of the final version of this article. JW, ML, XYuan and XYu revised the manuscript. JW and ML confirm the authenticity of all the raw data. All authors had no reservations and have read and approved the publication of the final version.

Ethics approval and participation consent

The present study was conducted as per the approval and regulations of the Ethics and Animal Research Committee of Huazhong University of Science and Technology [(2021) IACUC no. 2908].

Patient consent for publication

Not applicable.

Competing interests

The authors declare that they have no competing interests.

References

1. Wang BW, Jiang Y, Yao ZL, Chen PS, Yu B and Wang SN: Aucubin protects chondrocytes against IL-1β-induced apoptosis in vitro and inhibits osteoarthritis in mice model. Drug Des Devel Ther 13: 3529-3538, 2019.
2. Cui J, Shibata Y, Zhu T, Zhou J and Zhang J: Osteocytes in bone aging: Advances, challenges, and future perspectives. Ageing Res Rev 77: 101608, 2022.
3. Glyn-Jones S, Palmer AJ, Agricola R, Price AJ, Vincent TL, Weinans H and Carr AJ: Osteoarthritis. Lancet 386: 376-387, 2015.
4. Wu Y, Wang Z, Fu X, Lin Z and Yu K: Geraniol-mediated osteoarthritis improvement by down-regulating PI3K/Akt/NF-κB and MAPK signals: In vivo and in vitro studies. Int Immunopharmacol 86: 106713, 2020.
5. Rannou F, Pelletier JP and Martel-Pelletier J: Efficacy and safety of topical NSAIDs in the management of osteoarthritis: Evidence from real-life setting trials and surveys. Semin Arthritis Rheum 45: S18-21, 2016.
6. Schurman DJ and Smith RL: Osteoarthritis: Current treatment and future prospects for surgical, medical, and biologic intervention. Clin Orthop Relat Res (427 Suppl): S183-S189, 2004.
7. Cho Y, Jeong S, Kim H, Kang D, Lee J, Kang SB and Kim JH: Disease-modifying therapeutic strategies in osteoarthritis: Current status and future directions. Exp Mol Med 53: 1689-1696, 2021.
8. Zou K, Wong J, Abdullah N, Chen X, Smith T, Doherty M and Zhang W: Examination of overall treatment effect and the proportion attributable to contextual effect in osteoarthritis: Meta-analysis of randomised controlled trials. Ann Rheum Dis 75: 1964-1970, 2016.
9. Ni B, Pei W, Qu Y, Zhang R, Chu X, Wang Y, Huang X and You H: MCC950, the NLRP3 inhibitor, protects against cartilage degradation in a mouse model of osteoarthritis. Oxid Med Cell Longev 2021: 4139048, 2021.
10. Zhang H, Li J, Xiang X, Zhou B, Zhao C, Wei Q, Sun Y, Chen J, Lai B, Luo Z and Li A: Tert-butylhydroquinone attenuates osteoarthritis by protecting chondrocytes and inhibiting macrophage polarization. Bone Joint Res 10: 704-713, 2021.
11. Zhou S, Shi J, Wen H, Xie W, Han X and Li H: A chondroprotective effect of moracin on IL-1β-induced primary rat chondrocytes and an osteoarthritis rat model through Nrf2/HO-1 and NF-κB axes. Food Funct 11: 7935-7945, 2020.
12. Xu L, Wu Z, He Y, Chen Z, Xu K, Yu W, Fang W, Ma C, Moqbel SAA, Ran J, *et al*: MFN2 contributes to metabolic disorders and inflammation in the aging of rat chondrocytes and osteoarthritis. Osteoarthritis Cartilage 28: 1079-1091, 2020.
13. Cao Y, Tang S, Nie X, Zhou Z, Ruan G, Han W, Zhu Z and Ding C: Decreased miR-214-3p activates NF-κB pathway and aggravates osteoarthritis progression. EBioMedicine 65: 103283, 2021.
14. Chang SH, Mori D, Kobayashi H, Mori Y, Nakamoto H, Okada K, Taniguchi Y, Sugita S, Yano F, Chung UI, *et al*: Excessive mechanical loading promotes osteoarthritis through the gremlin-1-NF-κB pathway. Nat Commun 10: 1442, 2019.
15. Zhang C, Shao Z, Hu X, Chen Z, Li B, Jiang R, Bsoul N, Chen J, Xu C and Gao W: Inhibition of PI3K/Akt/NF-kappaB signaling by Aloin for ameliorating the progression of osteoarthritis: In vitro and in vivo studies. Int Immunopharmacol 89: 107079, 2020.
16. Huang X, Xi Y, Mao Z, Chu X, Zhang R, Ma X, Ni B, Cheng H and You H: Vanillic acid attenuates cartilage degeneration by regulating the MAPK and PI3K/AKT/NF-κB pathways. Eur J Pharmacol 859: 172481, 2019.
17. Nieminen R, Korhonen R, Moilanen T, Clark AR and Moilanen E: Aurothiomalate inhibits cyclooxygenase 2, matrix metalloproteinase 3, and interleukin-6 expression in chondrocytes by increasing MAPK phosphatase 1 expression and decreasing p38 phosphorylation: MAPK phosphatase 1 as a novel target for antirheumatic drugs. Arthritis Rheum 62: 1650-1659, 2010.
18. Moon TC, Murakami M, Kudo I, Son KH, Kim HP, Kang SS and Chang HW: A new class of COX-2 inhibitor, rutaecarpine from Evodia rutaecarpa. Inflamm Res 48: 621-625,1999.
19. Zhang Y, Yan T, Sun D, Xie C, Wang T, Liu X, Wang J, Wang Q, Luo Y, Wang P, *et al*: Rutaecarpine inhibits KEAP1-NRF2 interaction to activate NRF2 and ameliorate dextran sulfate sodium-induced colitis. Free Radic Biol Med 148: 33-41, 2020.
20. Woo HG, Lee CH, Noh MS, Lee JJ, Jung YS, Baik EJ, Moon CH and Lee SH: Rutaecarpine, a quinazolinocarboline alkaloid, inhibits prostaglandin production in RAW264.7 macrophages. Planta Med 67: 505-509, 2001.
21. Jayakumar T, Lin KC, Chang CC, Hsia CW, Manubolu M, Huang WC, Sheu JR and Hsia CH: Targeting MAPK/NF-κB Pathways in Anti-Inflammatory Potential of Rutaecarpine: Impact on Src/FAK-Mediated Macrophage Migration. Int J Mol Sci 23, 2021.
22. Guo B, Zhao C, Zhang C, Xiao Y, Yan G, Liu L and Pan H: Elucidation of the anti-inflammatory mechanism of Er Miao San by integrative approach of network pharmacology and experimental verification. Pharmacol Res 175: 106000, 2022.
23. Han M, Hu L and Chen Y: Rutaecarpine may improve neuronal injury, inhibits apoptosis, inflammation and oxidative stress by regulating the expression of ERK1/2 and Nrf2/HO-1 pathway in rats with cerebral ischemia-reperfusion injury. Drug Des Devel Ther 13: 2923-2931, 2019.
24. Fukuma Y, Sakai E, Komaki S, Nishishita K, Okamoto K and Tsukuba T: Rutaecarpine attenuates osteoclastogenesis by impairing macrophage colony stimulating factor and receptor activator of nuclear factor κ-B ligand-stimulated signalling pathways. Clin Exp Pharmacol Physiol 45: 863-865, 2018.
25. Jing S, Wan J, Wang T, He Z, Ding Q, Sheng G, Wang S, Zhao H, Zhu Z, Wu H and Li W: Flavokawain A alleviates the progression of mouse osteoarthritis: An in vitro and in vivo study. Front Bioeng Biotechnol 10: 1071776, 2022.
26. Livak KJ and Schmittgen TD: Analysis of relative gene expression data using real-time quantitative PCR and the 2(-Delta Delta C(T)) method. Methods 25: 402-408, 2001.
27. John SP, Singh A, Sun J, Pierre MJ, Alsalih L and Lipsey C: Small-molecule screening identifies Syk kinase inhibition and rutaecarpine as modulators of macrophage training and SARS-CoV-2 infection. Cell Rep 41: 111441, 2022.
28. McAlindon T: Osteoarthritis research society international (OARSI) Classification and Guidelines. HSS J 8: 66-67, 2012.
29. Sun K, Luo J, Jing X, Xiang W, Guo J, Yao X, Liang S, Guo F and Xu T: Hyperoside ameliorates the progression of osteoarthritis: An in vitro and in vivo study. Phytomedicine 80: 153387, 2021.
30. Lepetsos P, Papavassiliou KA and Papavassiliou AG: Redox and NF-κB signaling in osteoarthritis. Free Radic Biol Med 132: 90-100, 2019.
31. Maki K, Nava MM, Villeneuve C, Chang M, Furukawa KS, Ushida T and Wickstrom SA: Hydrostatic pressure prevents chondrocyte differentiation through heterochromatin remodeling. J Cell Sci 134: jcs247643, 2021.
32. Attur MG, Dave MN, Clancy RM, Patel IR, Abramson SB and Amin AR: Functional genomic analysis in arthritis-affected cartilage: Yin-yang regulation of inflammatory mediators by alpha 5 beta 1 and alpha V beta 3 integrins. J Immunol 164: 2684-2691, 2000.
33. Haugh MG, Vaughan TJ and Mcnamara LM: The role of integrin α(V)β(3) in Osteocyte mechanotransduction. J Mech Behav Biomed Mater 42:67-75, 2015.
34. Wang Q, Onuma K, Liu C, Wong H, Bloom MS, Elliott EE, Cao RR, Hu N, Lingampalli N, Sharpe O, *et al*: Dysregulated integrin alphaVbeta3 and CD47 signaling promotes joint inflammation, cartilage breakdown, and progression of osteoarthritis. JCI Insight 4: e128616, 2019.
35. Wang Z, Boyko T, Tran MC, LaRussa M, Bhatia N, Rashidi V, Longaker MT and Yang GP: DEL1 protects against chondrocyte apoptosis through integrin binding. J Surg Res 231: 1-9, 2018.
36. Lu R, Yu X, Liang S, Cheng P, Wang Z, He ZY, Lv ZT, Wan JL, Mo H, Zhu WT, and Chen AM: Physalin A Inhibits MAPK and NF-κB signal transduction through integrin αVβ3 and exerts chondroprotective effect. Front Pharmacol 12: 761922, 2021.
37. Cheng C, Tian J, Zhang F, Deng Z, Tu M, Li L, Yang H, Xiao K, Guo W, Yang RQ, *et al*: WISP1 protects against chondrocyte senescence and apoptosis by regulating αvβ3 and PI3K/Akt pathway in osteoarthritis. DNA Cel Biol 40: 629-637, 2021.
38. Emami A, Tepper J, Short B, Yaksh TL, Bendele AM, Ramani T, Cisternas AF, Chang GH and Mellon RD: Toxicology evaluation of drugs administered via uncommon routes: Intranasal, intraocular, intrathecal/intraspinal, and intra-articular. Int J Toxicol 37: 4-27, 2018.